

Photonic Bandgap Calculations Using Dirichlet-to-Neumann Maps

Jianhua Yuan

*Department of Mathematics
Beijing University of Posts and Telecommunications
Beijing, China*

Ya Yan Lu

*Department of Mathematics
City University of Hong Kong
Kowloon, Hong Kong
mayylu@cityu.edu.hk*

A simple and efficient method for computing bandgap structures of two dimensional photonic crystals is presented in this paper. Using the Dirichlet-to-Neumann (DtN) map of the unit cell, the bandgaps are calculated as an eigenvalue problem for each given frequency, where the eigenvalue is related to the Bloch wave vector. A linear matrix eigenvalue problem is obtained even when the medium is dispersive. For photonic crystals composed of a square lattice of parallel cylinders, the DtN map is obtained by a cylindrical wave expansion. This leads to eigenvalue problems for relatively small matrices. Unlike other methods based on cylindrical wave expansions, sophisticated lattice sums techniques are not needed. © 2006 Optical Society of America

OCIS codes: 000.4430,260.2110

1. Introduction

Photonic crystals^{1,2} have been extensively studied due to their unusual ability to manipulate the flow of light. Many useful applications of photonic crystals have been proposed and realized. Efficient numerical methods are needed to understand the basic properties of photonic crystals and to design and optimize related devices. Starting from the late 80's, many numerical methods have been developed to analyze photonic crystals and related structures. Both frequency-domain and time-domain methods are used to compute bandgap structures,

defect modes, waveguide modes, and to simulate lightwaves in more complicated photonic crystal structures, such as bends, branches, etc.

The most important property of a photonic crystal is its bandgap structure. Current methods for computing bandgap structures include the plane-wave expansion method,³⁻⁷ cylindrical/spherical wave expansion (CWE) method,⁸⁻¹⁰ the transfer matrix method,^{11,12} the scattering matrix method,¹³ the finite difference method,¹⁴⁻¹⁶ the finite element method,^{17,18} the finite difference time domain (FDTD) method,¹⁹⁻²¹ the multiple multipole method,²² the cell method,²³ the moving least-squares method,²⁴ the wavelet method,²⁵ etc. In the frequency domain, the standard formulation¹ gives rise to an eigenvalue problem, where ω^2 is the eigenvalue. For a non-dispersive medium, this is a linear eigenvalue problem. When it is discretized, we obtain a standard matrix eigenvalue problem. The discretization can be achieved by discretizing a unit cell of the photonic crystal, for example, by the finite element method^{17,18} and the finite difference method.¹⁴⁻¹⁶ The “discretization” can also be achieved by expanding the eigenfunction in some series,²⁶ such as the Fourier series in the plane-wave expansion method.³⁻⁷ The linear eigenvalue problems (for non-dispersive media) can also be turned to nonlinear eigenvalue problems as in the CWE method.⁸⁻¹⁰ The nonlinear approach is useful, since it gives rise to much smaller matrices. However, the eigenvalue ω^2 must be searched one-by-one from the condition that a matrix becomes singular. For dispersive media, the original eigenvalue problem itself becomes nonlinear. In the CWE method, the lattice Green’s function is involved and its evaluation requires lattice sums techniques. In the transfer matrix method^{11,12} and the scattering matrix method,¹³ the bandgap problem is formulated as an eigenvalue problem, where the eigenvalue is a function of the Bloch wave vector. These methods give rise to linear eigenvalue problems even when the medium is dispersive. Due to the difficulty with evanescent modes in the transfer matrix method, the scattering matrix method is preferred. How the scattering (or transfer) matrix is obtained is a separate problem. For example, many existing numerical methods for diffractive optics can be used to compute the scattering matrix. In particular, the cylindrical wave expansion method can be used, but a sophisticated lattice sums technique is again required.

In this paper, we develop a Dirichlet-to-Neumann (DtN) map method for computing bandgap structures of two-dimensional photonic crystals. The DtN map is an operator that maps the wave field on the boundary of a unit cell to its normal derivative there. Like the transfer matrix and the scattering matrix methods, we obtain a linear eigenvalue problem even for a dispersive medium, where the eigenvalue is related to the Bloch wave vector. The computation of DtN map is also a separate problem. Our approach is to use a cylindrical wave expansion. This gives rise to accurate approximations of the DtN map with matrices of very small size. Compared with the scattering matrix method,¹³ our method is much simpler, since lattice sums techniques are not needed.

The outline of the remainder of this paper is as follows. In section 2, we develop a matrix approximation to the DtN map using cylindrical wave expansions. In section 3, we formulate the eigenvalue problem using the DtN map and describe an efficient method for computing the bandgaps directly. Numerical examples are given in section 4. We have computed dispersion relations and gap maps for two-dimensional photonic crystals composed of a square lattice of circular cylinders for both dispersive and non-dispersive media.

2. Dirichlet-to-Neumann map of a unit cell

In a two-dimensional medium which is invariant in the z -direction, the governing equations are

$$\frac{\partial^2 u}{\partial x^2} + \frac{\partial^2 u}{\partial y^2} + k_0^2 n^2 u = 0 \quad (1)$$

for the E polarization and

$$\frac{\partial}{\partial x} \left(\frac{1}{n^2} \frac{\partial u}{\partial x} \right) + \frac{\partial}{\partial y} \left(\frac{1}{n^2} \frac{\partial u}{\partial y} \right) + k_0^2 u = 0 \quad (2)$$

for the H polarization, where k_0 is the free space wavenumber, $n = n(x, y)$ is the refractive index, u is the z -component (the only non-zero component) of the electric or magnetic fields for the E or H polarizations, respectively. For a square lattice with a lattice constant L , the refractive index n satisfies

$$n(x, y) = n(x + m_1 L, y + m_2 L) \quad (3)$$

for any integers m_1 and m_2 . The Dirichlet-to-Neumann (DtN) map is the operator Λ that maps u on the boundary of the square unit cell to the normal derivative of u on the boundary. A matrix approximation to Λ is needed in our method for computing bandgap structures of the photonic crystal.

For photonic crystals composed of a square lattice of circular cylinders, the DtN map Λ can be efficiently calculated by a cylindrical wave expansion. For a square unit cell given by $0 < x < L$ and $0 < y < L$ and assuming that a cylinder is located at the center of the unit cell, we have $n = n_1$ for $r < a$ and $n = n_2$ for $r > a$, where r and θ are the polar coordinates such that $r = 0$ corresponds to $x = y = L/2$, a is the radius of the cylinder, n_1 and n_2 are the refractive indices of the cylinder and the surrounding medium, respectively. Under these assumptions, the Helmholtz equations (1) and (2) have the following general solutions

$$u(x, y) = \sum_{m=-\infty}^{\infty} C_m \Phi_m(r, \theta), \quad \Phi_m(r, \theta) = \phi_m(r) e^{im\theta}, \quad (4)$$

where $\phi_m(r)$ is related to the Bessel functions J_m and Y_m as

$$\phi_m(r) = \begin{cases} A_m J_m(k_0 n_1 r), & r < a; \\ B_m J_m(k_0 n_2 r) + Y_m(k_0 n_2 r), & r > a. \end{cases}$$

In the above, the coefficient of Y_m is arbitrarily scaled to be 1. The coefficients A_m and B_m can be solved from the interface conditions at $r = a$. We have

$$\begin{aligned} A_m J_m(k_0 n_1 a) - B_m J_m(k_0 n_2 a) &= Y_m(k_0 n_2 a), \\ \frac{n_1}{n_2} A_m J'_m(k_0 n_1 a) - B_m J'_m(k_0 n_2 a) &= Y'_m(k_0 n_2 a) \end{aligned}$$

for the E polarization and

$$\begin{aligned} A_m J_m(k_0 n_1 a) - B_m J_m(k_0 n_2 a) &= Y_m(k_0 n_2 a), \\ \frac{n_2}{n_1} A_m J'_m(k_0 n_1 a) - B_m J'_m(k_0 n_2 a) &= Y'_m(k_0 n_2 a) \end{aligned}$$

for the H polarization. Using the general solution (4), it is possible to find the DtN map Λ of the unit cell satisfying

$$\Lambda \begin{bmatrix} u_0 \\ v_0 \\ u_1 \\ v_1 \end{bmatrix} = \begin{bmatrix} \partial_y u_0 \\ \partial_x v_0 \\ \partial_y u_1 \\ \partial_x v_1 \end{bmatrix}, \quad (5)$$

where u_0, u_1, v_0 and v_1 are restrictions of u on the four edges of the square:

$$u_0 = u(x, 0), \quad u_1 = u(x, L), \quad v_0 = u(0, y), \quad v_1 = u(L, y)$$

and

$$\partial_y u_0 = \partial_y u|_{y=0}, \quad \partial_y u_1 = \partial_y u|_{y=L}, \quad \partial_x v_0 = \partial_x u|_{x=0}, \quad \partial_x v_1 = \partial_x u|_{x=L}.$$

In the discrete case, we select N points on each edge of the square corresponding to

$$x_j = y_j = (j - 0.5) \frac{L}{N}, \quad j = 1, 2, \dots, N$$

and replace u_0, u_1, v_0 and v_1 by column vectors of length N , then the DtN map Λ is approximated by a $(4N) \times (4N)$ matrix. More precisely, we first truncate (4) as

$$u(x, y) = \sum_{m=-2N}^{2N-1} C_m \Phi_m(r, \theta), \quad (6)$$

then evaluate u at the $4N$ points on the boundary. This gives rise to a matrix Λ_1 that maps the coefficients $\{C_m\}$ to the $4N$ values of u on the boundary. Similarly, if we evaluate the normal derivative of u (which are just partial derivatives with respect to x or y here) at these $4N$ points by (6), we obtain a matrix Λ_2 that maps $\{C_m\}$ to the normal derivatives. Therefore, we obtain the following matrix approximation of the DtN map:

$$\Lambda = \Lambda_2 \Lambda_1^{-1}. \quad (7)$$

The number of operations required to compute Λ is $O(N^3)$.

Notice that the infinite cylindrical wave expansion (4) converges only when $r < L - a$ (the distance from the center of a cylinder to the edges of the nearby cylinders) and this region does not always include the entire square unit cell, but the finite sum (6) is always an exact solution on the entire unit cell.

3. The eigenvalue problem

For a two-dimensional photonic crystal, we consider the Bloch mode solutions of the Helmholtz equation (1) or (2) given by

$$u(x, y) = e^{i(\alpha x + \beta y)} \Psi(x, y), \quad (8)$$

where (α, β) is the Bloch wave vector and Ψ follows the same periodic condition (3) as the refractive index function. For a square lattice, the periodicity of the structure in the x and y directions leads to

$$u(x, L) = \rho_\beta u(x, 0), \quad \frac{\partial u(x, L)}{\partial y} = \rho_\beta \frac{\partial u(x, 0)}{\partial y}, \quad (9)$$

$$u(L, y) = \rho_\alpha u(0, y), \quad \frac{\partial u(L, y)}{\partial x} = \rho_\alpha \frac{\partial u(0, y)}{\partial x}, \quad (10)$$

where L is the lattice constant, $\rho_\beta = e^{i\beta L}$ and $\rho_\alpha = e^{i\alpha L}$. In the standard formulation,¹ the bandgap problem is an eigenvalue problem for given α and β , where ω^2 ($\omega = k_0 c$ is the angular frequency, c is the speed of light in vacuum) is the eigenvalue. For a non-dispersive medium, this is a linear eigenvalue problem, but it becomes a nonlinear eigenvalue problem when the medium is dispersive (i.e. n varies with ω). In the following, we formulate the bandgap problem as an eigenvalue problem for a given ω , where the eigenvalue is related to α and β .

For the square unit cell $0 < x < L$ and $0 < y < L$, we have the DtN map Λ satisfying (5). The operator Λ can be naturally partitioned as 4×4 blocks. This leads to

$$\begin{bmatrix} \Lambda_{11} & \Lambda_{12} & \Lambda_{13} & \Lambda_{14} \\ \Lambda_{21} & \Lambda_{22} & \Lambda_{23} & \Lambda_{24} \\ \Lambda_{31} & \Lambda_{32} & \Lambda_{33} & \Lambda_{34} \\ \Lambda_{41} & \Lambda_{42} & \Lambda_{43} & \Lambda_{44} \end{bmatrix} \begin{bmatrix} u_0 \\ v_0 \\ u_1 \\ v_1 \end{bmatrix} = \begin{bmatrix} \partial_y u_0 \\ \partial_x v_0 \\ \partial_y u_1 \\ \partial_x v_1 \end{bmatrix}. \quad (11)$$

If we write down the four equations in (11) and apply the periodic conditions (9) and (10), we can eliminate $u_1, v_1, \partial_y u_0, \partial_x v_0, \partial_y u_1$ and $\partial_x v_1$, and obtain

$$\begin{bmatrix} \Lambda_{31} & \Lambda_{32} \\ \Lambda_{41} & \Lambda_{42} \end{bmatrix} \begin{bmatrix} u_0 \\ v_0 \end{bmatrix} = \begin{bmatrix} M_{11} & M_{12} \\ M_{13} & M_{14} \end{bmatrix} \begin{bmatrix} u_0 \\ v_0 \end{bmatrix} \quad (12)$$

where $M_{11}, M_{12}, M_{21}, M_{22}$ are operators given by

$$\begin{aligned}
M_{11} &= \rho_\beta^2 \Lambda_{13} + \rho_\beta (\Lambda_{11} - \Lambda_{33}), \\
M_{12} &= \rho_\beta \rho_\alpha \Lambda_{14} - \rho_\alpha \Lambda_{34} + \rho_\beta \Lambda_{12}, \\
M_{21} &= \rho_\beta \rho_\alpha \Lambda_{23} + \rho_\alpha \Lambda_{21} - \rho_\beta \Lambda_{43}, \\
M_{22} &= \rho_\alpha^2 \Lambda_{24} + \rho_\alpha (\Lambda_{22} - \Lambda_{44}).
\end{aligned}$$

In general, we seek dispersion relationships for (α, β) in the irreducible Brillouin zone. For a square lattice of circular cylinders, this is the triangular region with corners at the Γ ($\alpha = \beta = 0$), X ($\alpha = 0, \beta = \pi/L$) and M ($\alpha = \beta = \pi/L$) points. In most bandgap calculations, the dispersion relationships are only calculated for (α, β) on the boundary of the irreducible Brillouin zone. If (α, β) is varied along the edges of the triangle ΓXM , we have $\rho_\beta = 1$ from Γ to X , $\rho_\alpha = -1$ from X to M and $\rho_\alpha = \rho_\beta$ from M to Γ . In all these three cases, equation (12) can be written as

$$(\lambda^2 \mathcal{A} + \lambda \mathcal{B} + \mathcal{C}) \mathbf{U} = 0, \quad (13)$$

where $\mathbf{U} = (u_0, v_0)^T$, the operators $\mathcal{A}, \mathcal{B}, \mathcal{C}$ and the scalar λ are defined on each edge of the irreducible Brillouin zone as follows:

1. From Γ to X , $\lambda = e^{i\alpha L}$ for $0 < \alpha \leq \pi/L$ and

$$\begin{aligned}
\mathcal{A} &= \begin{bmatrix} 0 & 0 \\ 0 & -\Lambda_{24} \end{bmatrix}, \quad \mathcal{B} = \begin{bmatrix} 0 & \Lambda_{34} - \Lambda_{14} \\ -\Lambda_{21} - \Lambda_{23} & \Lambda_{44} - \Lambda_{22} \end{bmatrix}, \\
\mathcal{C} &= \begin{bmatrix} \Lambda_{31} - \Lambda_{13} + \Lambda_{33} - \Lambda_{11} & \Lambda_{32} - \Lambda_{12} \\ \Lambda_{41} + \Lambda_{43} & \Lambda_{42} \end{bmatrix};
\end{aligned} \quad (14)$$

2. From X to M , $\lambda = e^{i\beta L}$ for $0 < \beta \leq \pi/L$ and

$$\begin{aligned}
\mathcal{A} &= \begin{bmatrix} -\Lambda_{13} & 0 \\ 0 & 0 \end{bmatrix}, \quad \mathcal{B} = \begin{bmatrix} \Lambda_{33} - \Lambda_{11} & \Lambda_{14} - \Lambda_{12} \\ \Lambda_{43} + \Lambda_{23} & 0 \end{bmatrix}, \\
\mathcal{C} &= \begin{bmatrix} \Lambda_{31} & \Lambda_{32} - \Lambda_{34} \\ \Lambda_{41} + \Lambda_{21} & \Lambda_{42} - \Lambda_{24} + \Lambda_{22} - \Lambda_{44} \end{bmatrix};
\end{aligned} \quad (15)$$

3. From M to Γ , $\lambda = e^{i\alpha L} = e^{i\beta L}$, ($0 \leq \alpha = \beta \leq \pi/L$) and

$$\begin{aligned}
\mathcal{A} &= \begin{bmatrix} -\Lambda_{13} & -\Lambda_{14} \\ -\Lambda_{23} & -\Lambda_{24} \end{bmatrix}, \quad \mathcal{B} = \begin{bmatrix} \Lambda_{33} - \Lambda_{11} & \Lambda_{34} - \Lambda_{12} \\ \Lambda_{43} - \Lambda_{21} & \Lambda_{44} - \Lambda_{22} \end{bmatrix}, \\
\mathcal{C} &= \begin{bmatrix} \Lambda_{31} & \Lambda_{32} \\ \Lambda_{41} & \Lambda_{42} \end{bmatrix}.
\end{aligned} \quad (16)$$

This is a quadratic eigenvalue problem, since a nonzero solution of \mathbf{U} only exists for special values of λ (the eigenvalues). In bandgap calculations, we are concerned with real α and β (for propagating Bloch waves), therefore, we only need to calculate eigenvalues that stay on the unit circle. The classical approach to solve quadratic eigenvalue problems of the form (13) is to perform a linearization. By introducing the vector $\mathbf{V} = \lambda\mathbf{U}$, the quadratic eigenvalue problem (13) is reduced to

$$\lambda \begin{bmatrix} \mathcal{A} & 0 \\ 0 & I \end{bmatrix} \begin{bmatrix} \mathbf{V} \\ \mathbf{U} \end{bmatrix} + \begin{bmatrix} \mathcal{B} & \mathcal{C} \\ -I & 0 \end{bmatrix} \begin{bmatrix} \mathbf{V} \\ \mathbf{U} \end{bmatrix} = 0, \quad (17)$$

where I is the identity operator. This linear eigenvalue problem can be solved with standard linear algebra programs.²⁷

In the discrete case, all operators are represented by matrices. If $x \in (0, L)$ and $y \in (0, L)$ are discretized by N points, the operators Λ_{ij} are approximated by $N \times N$ matrices. Therefore, equation (17) is a generalized eigenvalue problem of $(4N) \times (4N)$ matrices and it can be solved in $O(N^3)$ operations.

4. Numerical examples

To validate our method, we consider some numerical examples in this section. As usual, we show dispersion curves with the Bloch wave vector (α, β) given on the boundary of the irreducible Brillouin zone. Our method is especially suitable for computing the bandgaps directly. This will be illustrated in our calculations of gap maps.

For the first example, we consider a square lattice of identical dielectric cylinders in vacuum. The dielectric constant of the cylinders is $\epsilon_1 = n_1^2 = 8.9$. The radius of the cylinders is $a = 0.378L$, where L is the lattice constant. Using 9 points on each edge of the unit cell, i.e., $N = 9$, we obtain the dispersion curves for both polarizations. The eigenvalue problem (17) involves 36×36 matrices. The results for the E polarization are given in Fig. 1. The ordinate is the normalized frequency $\omega L / (2\pi c)$, where ω is the angular frequency and c is the speed of light in vacuum. The abscissa is the edge of the irreducible Brillouin zone. Our results are identical to the finite element results reported in Ref. 17, where the unit cell is discretized with 4096 elements (leading to eigenvalue problems of 4096×4096 matrices). To obtain the dispersion curves, we solve the eigenvalue problem (17) for various values of ω . Since the eigenvalue λ is related to the Bloch wave vector (α, β) by $\lambda = e^{i\alpha L}$ or $\lambda = e^{i\beta L}$, those eigenvalues on the unit circle (i.e. $|\lambda| = 1$) are saved for each ω . In practice, we replace the condition $|\lambda| = 1$ by $|1 - |\lambda|| \leq 10^{-6}$. On each edge of the irreducible Brillouin zone, the saved eigenvalues are further organized as sequences where each sequence corresponds to one dispersion curve. This can be achieved by imposing the continuity of the derivative of the dispersion curves. Since the dispersion curves may become very flat at some frequencies, a

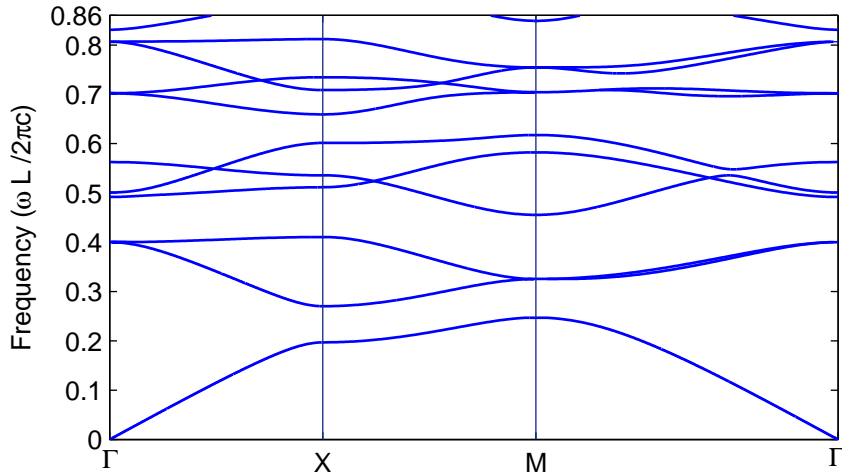


Fig. 1. Computed band structure for Example 1: the E polarization.

small increment of ω may be needed. To improve the efficiency, an adaptive procedure that links the increment of ω with the slopes of the dispersion curves can be used.

Our method is especially suitable for computing the bandgaps directly, that is, without computing the detailed dispersion curves first. It turns out that the eigenvalues of (17) appear in pairs as λ and $1/\lambda$. That is, if λ is an eigenvalue of (17), then so is $1/\lambda$. Since the dispersion curves correspond to eigenvalues on the unit circle, we can calculate the shortest distance to the unit circle among all eigenvalues satisfying $|\lambda| \leq 1$. That is,

$$F(\omega) = \min\{|1 - |\lambda||, \lambda \text{ is an eigenvalue of (17) and } |\lambda| \leq 1\}.$$

The eigenvalues for three different edges of the irreducible Brillouin zone are all included in the above definition. Clearly, if ω is in a bandgap, then $F(\omega) > 0$, otherwise $F(\omega) = 0$. The bandgaps can be calculated by searching intervals of ω where $F(\omega) > 0$. For this purpose, we have implemented a simple bisection method that determines the end points of such intervals. Using this method, we calculate the gap map for the above square lattice of cylinders with $\epsilon_1 = 8.9$. As shown in Fig. 2, the gap map reveals the dependence of the bandgaps on the ratio between the radius of the cylinders and the lattice constant.

For a dispersive medium, our method remains unchanged. The eigenvalue problem (17) is linear even when the medium is dispersive. As the second example, we consider the square lattice of dispersive circular cylinders studied in Ref. 21 and Ref. 20. The dielectric constant

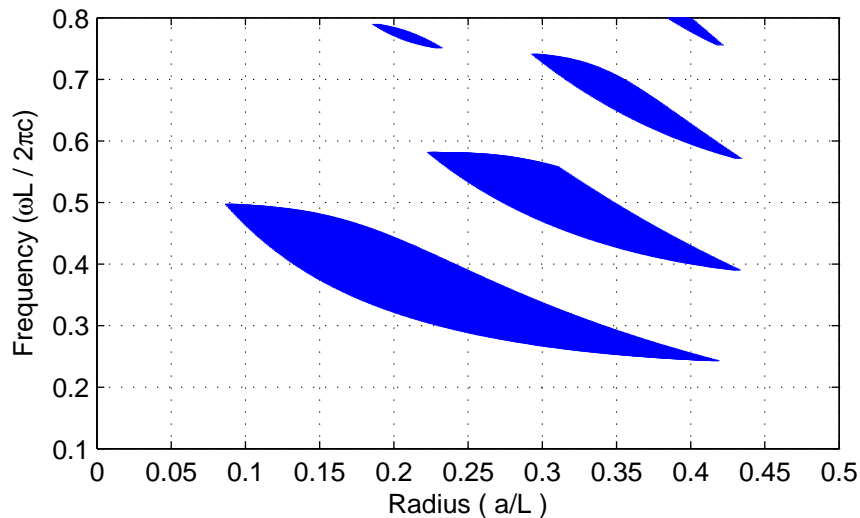


Fig. 2. The gap map of the E polarization for Example 1.

of the cylinders is assumed to satisfy

$$\epsilon_1(\omega) = \epsilon_\infty \left(1 - \frac{\omega_p^2}{\omega^2}\right), \quad (18)$$

where ω_p is the plasma frequency and ϵ_∞ is the dielectric constant for infinite frequency. For the E polarization, we choose

$$\epsilon_\infty = 1, \quad a = 0.472L, \quad \omega_p = \frac{2\pi c}{L},$$

where L is the lattice constant and a is the radius of the cylinders. The dispersion curves for the E polarization are shown in Fig. 3. For other values of a/L , the bandgaps are shown in Fig. 4. For the H polarization, our method requires very little modification. As in Refs. 21 and 20, we choose

$$\epsilon_\infty = 1, \quad a = 0.3L, \quad \omega_p = \frac{2\pi c}{L}$$

and obtain the dispersion curves in Fig. 5. These numerical results are obtained with $N = 9$. They are identical to the FDTD results reported in Refs. 21 and 20.

For metallic cylinders, the dielectric constant ϵ_1 should have an imaginary part, for example, as given in the Drude model:

$$\epsilon_1(\omega) = \epsilon_\infty \left[1 - \frac{\omega_p^2}{(\omega + i\delta)(\omega + i\gamma)}\right],$$

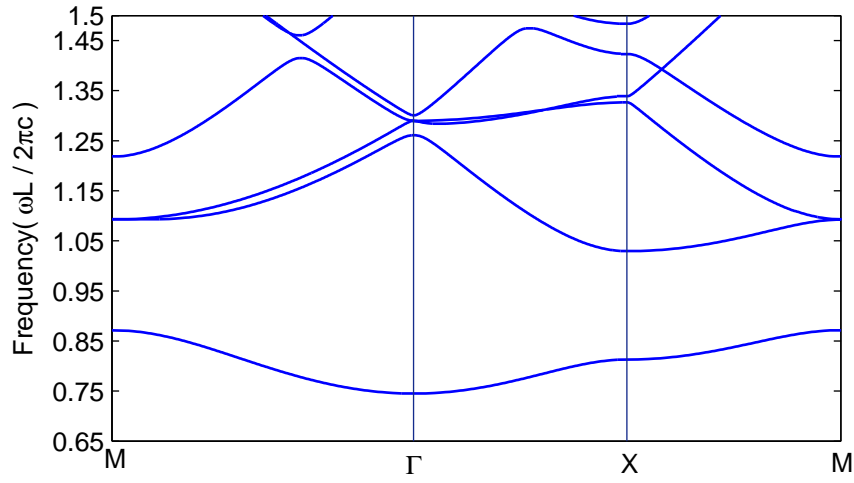


Fig. 3. Computed band structure for Example 2: the E polarization.

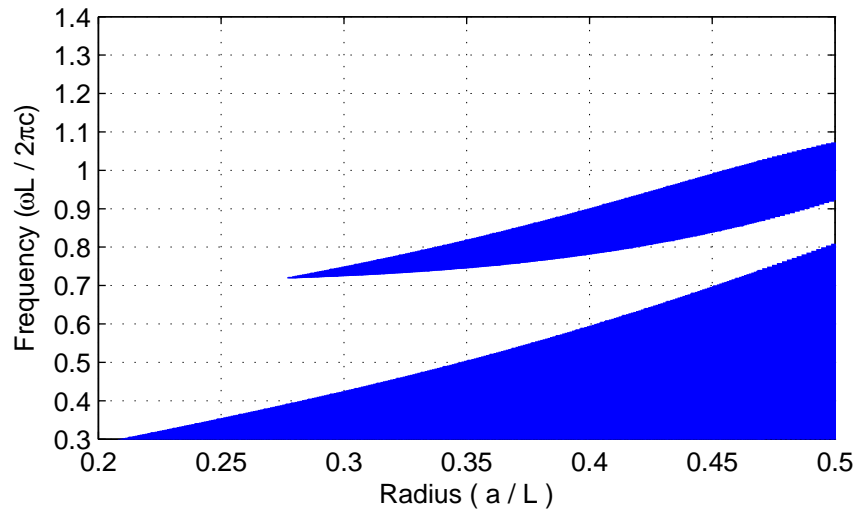


Fig. 4. The gap map of the E polarization for Example 2.

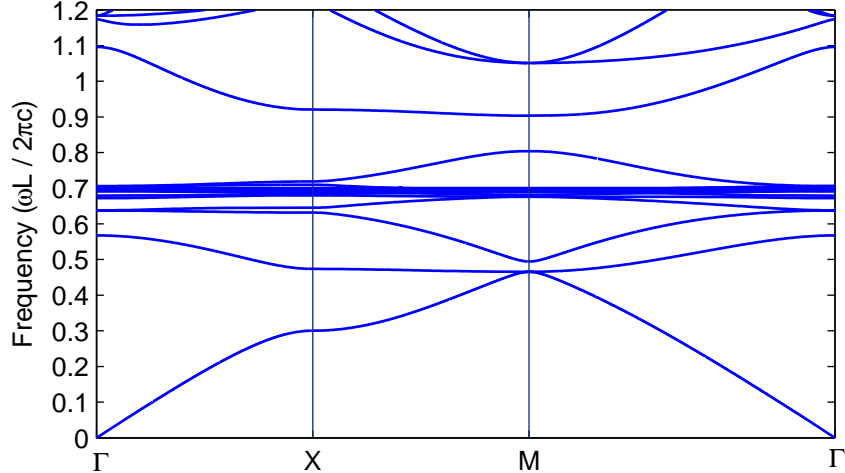


Fig. 5. Computed band structure for Example 2: the H polarization.

where γ is the relaxation rate and δ is a positive infinitesimal. In this case, the differential operator in the standard eigenvalue formulation,¹ where ω^2 is the eigenvalue, is not self-adjoint. Therefore, the eigenvalue ω^2 is in general complex for any given real Bloch wave vector (α, β) . In our formulation, a real ω is given as an input parameter, then α or β will have an imaginary part. The eigenvalue problem (17) can be solved without any difficulty, but the dispersion curves no longer correspond to $|\lambda| = 1$, where the eigenvalue λ is either $e^{i\alpha L}$ or $e^{i\beta L}$. As in Ref. 20, we choose to avoid the case of a complex dielectric constant by using the simpler model (18).

5. Conclusions

We have developed a Dirichlet-to-Neumann (DtN) map approach for computing bandgap structures of photonic crystals. For 2-D photonic crystals composed of circular cylinders, the DtN map can be efficiently calculated by cylindrical wave expansions. Our method avoids a discretization of the unit cell and it gives rise to linear eigenvalue problems of relatively small matrices even when the medium is dispersive. Unlike other methods based on cylindrical wave expansions, our method is simple to implement, since it does not require sophisticated lattice sums techniques.

Acknowledgments

This research was partially supported by a grant from the Research Grants Council of Hong Kong Special Administrative Region, China (Project No. CityU 101804).

References

1. J. D. Joannopoulos, R. D. Meade and J. N. Winn, *Photonic Crystals: Molding the Flow of Light*, Princeton University Press, Princeton, NJ. 1995.
2. K. Sakoda, *Optical Properties of Photonic Crystals*, Springer Verlag, Berlin, 2001.
3. K. M. Leung and Y. F. Liu, “Full vector wave calculation of photonic band structures in face-centered-cubic dielectric media”, *Phys. Rev. Lett.* **65**, 2646–2649 (1990).
4. Z. Zhang and S. Satpathy, “Electromagnetic wave propagation in periodic structures – Bloch wave solution of Maxwell’s equations”, *Phys. Rev. Lett.* **65**, 2650–2653 (1990).
5. K. M. Ho, C. T. Chan and C. M. Soukoulis, “Existence of a photonic gap in periodic dielectric structures”, *Phys. Rev. Lett.* **65**, 3152–3155 (1990).
6. R. D. Meade, A. M. Rappe, K. D. Brommer, J. D. Joannopoulos and O. L. Alerhand, “Accurate theoretical analysis of photonic band-gap materials”, *Phys. Rev. B* **48**, 8434–8437 (1993).
7. S. G. Johnson and J. D. Joannopoulos, “Block-iterative frequency-domain methods for Maxwell’s equations in a planewave basis”, *Opt. Express* **8**, 173–190 (2001).
8. K. M. Leung and Y. Qiu, “Multiple-scattering calculation of the two-dimensional photonic band structure”, *Phys. Rev. Lett.* **48**, 7767–7771 (1993).
9. N. A. Nicorovici and R. C. McPhedran, “Photonic band gaps for arrays of perfectly conducting cylinders”, *Phys. Rev. E* **52**, 1135–1145 (1995).
10. K. Ohtaka, T. Ueta and K. Amemiya, “Calculation of photonic bands using vector cylindrical waves and reflectivity of light for an array of dielectric rods”, *Phys. Rev. B* **57**, 2550–2568 (1998).
11. J. B. Pendry and A. MacKinnon, “Calculation of photon dispersion relations”, *Phys. Rev. Lett.* **69**, 2772–2775 (1992).
12. J. B. Pendry, “Calculating photonic band structure”, *Journal of Physics: Condensed Matter* **8**, 1085–1108 (1996).
13. L. C. Botten, N. A. Nicorovici, R. C. McPhedran, C. Martijn de Sterke and A. A. Asatryan, “Photonic band structure calculations using scattering matrices”, *Phys. Rev. E* **64**, 046603 (2001).
14. H. Y. D. Yang, “Finite difference analysis of 2-D photonic crystals”, *IEEE Trans. Microwave Theory Tech.* **44**, 2688–2695 (1996).

15. C. P. Yu and H. C. Chang, “Applications of the finite difference mode solution method to photonic crystal structures”, *Optical and Quantum Electronics* **36**, 145–163 (2004).
16. S. Guo, F. Wu, S. Albin and R. S. Rogowski, “Photonic band gap analysis using finite-difference frequency-domain method”, *Opt. Express* **12**, 1741–1746 (2004).
17. D. C. Dobson, “An efficient method for band structure calculations in 2D photonic crystals”, *J. Comput. Phys.* **149**, 363–379 (1999).
18. W. Axmann and P. Kuchment, “An efficient finite element method for computing spectra of photonic and acoustic band-gap materials: I. Scalar case”, *J. Comput. Phys.* **150**, 468–481 (1999).
19. C. T. Chan, Q. L. Yu and K. M. Ho, “Order-N spectral method for electromagnetic waves”, *Phys. Rev. B* **51**, 16635–16642 (1995).
20. K. Sakoda, N. Kawai, T. Ito, A. Chutinan, S. Noda, T. Mitsuyu and K. Hirao, “Photonic bands of metallic systems. I. Principle of calculation and accuracy”, *Phys. Rev. B* **64**, 045116 (2001).
21. T. Ito and K. Sakoda, “Photonic bands of metallic systems. II. Features of surface plasmon polaritons”, *Phys. Rev. B* **64**, 045117 (2001).
22. E. Moreno, D. Erni and C. Hafner, “Band structure computations of metallic photonic crystals with the multiple multipole method”, *Phys. Rev. B* **65**, 155120 (2002).
23. M. Marrone, V. F. Rodriguez-Esquerre and H. E. Hernández-Figueroa, “Novel numerical method for the analysis of 2D photonic crystals: the cell method”, *Opt. Express* **10**, 1299–1304 (2002).
24. S. Jun, Y. S. Cho and S. Im, “Moving least-square method for the band-structure calculation of 2D photonic crystals”, *Opt. Express* **11**, 541–551 (2003).
25. X. Checoury and J. M. Lourtioz, “Wavelet method for computing band diagrams of 2D photonic crystals”, *Opt. Commun.* **259**, 360–365 (2006).
26. A. Figotin and Y. A. Godin, “The computation of spectra of some 2D photonic crystals”, *J. Comput. Phys.* **136**, 585–598 (1997).
27. E. Anderson, Z. Bai, C. Bischof, S. Blackford, J. Demmel, J. Dongarra, J. Du Croz, A. Greenbaum, S. Hammarling, A. McKenney and D. Sorensen, *LAPACK Users’ Guides*, 3rd ed., Society for Industrial and Applied Mathematics, Philadelphia, 1999.